FEATURE ARTICLE

ChemComm
www.rsc.org/chemcomm

Cyclic molecular materials based on $[M_2O_2S_2]^{2+}$ cores (M = Mo or W)

Emmanuel Cadot and Francis Sécheresse

Institut Lavoisier. IREM, UMR 86378. Université de Versailles Saint Quentin, 45 Avenue des Etats-Unis, 78035 Versailles, France. E-mail: cadot@chimie.uvsq.fr

Received (in Cambridge, UK) 9th April 2002, Accepted 10th June 2002
First published as an Advance Article on the web 25th June 2002

The purpose of this article is to illustrate how conventional precursors can serve, when used with a drop of imagination, to the synthesis of sophisticated inorganic rings and wheels. The self-condensation of the $[M_2O_2S_2]^{2+}$ fragments under acido–basic process produces, in the presence or absence of guest species, linear enchainment restricted to discrete cyclic entities. This approach was revealed to be a highly fruitful strategy for developing an extended family of compounds, differing in their nuclearity, size and shape, and the nature of the encapsulated guest molecule. Indeed, the resulting cycles delimit a cationic open cavity, which can be filled by neutral polar molecules such as aquo ligands or anionic molecules such as phosphates, polycarboxylates and even metalates. The flexibility of the rings is at the origin of interesting host–guest properties: the deformation (symmetry) and the adaptation (nuclearity) of the inorganic cycle are directly related to the size and the coordination requirements of the encapsulated substrate. The versatility of the metal coordination, octahedral or square pyramidal, confers dynamic properties to the ring . In the solid state, molecular rings assemble in striking 3-D networks based on direct cation–anion connections. Alkali cations are arranged in pillars or layers for anchoring the anionic rings.

Introduction

Early transition-metal sulfides, especially those of V, Mo and W, represent a prominent class of compounds involved in many areas of chemistry.[1,2] In particular, such systems are studied extensively for their implications in biological[3,4] and industrial catalytic processes.[5,6] Metal–sulfide cluster anions, commonly referred to as thiometalates, exhibit topologies often limited to some archetypal architectures,[7] with low nuclearity rarely exceeding four metallic centers. These features contrast with anionic metal–oxygen combinations, namely the polyoxometalates (POMs). POMs are remarkable for their electronic and structural diversity and their relevance to diverse areas of science,[8] *e.g.* catalysis,[9] medicine[10] and materials.[11] Recently, such compounds have reached the nanometric scale as illustrated by spectacular examples such as the 'big wheel' for molybdenum blues[12] and the 'giant butterfly' for heteropolytungstates.[13] Thus, the domain of the POM chemistry has been for a long time clearly separated from that of thiometalates by the nature, size and shape, coordination and electronic properties of these compounds.[14] In the last decade, only few polyoxothiometalates of high nuclearity, at the boundary of these two fields, have been reported. These examples result from the direct sulfurization of niobium-containing POMs and have retained their Linqvist[15] or Keggin[16,17] parent architectures. On the other hand, we have pioneered another elegant approach, consisting in the stereospecific addition of a preformed thiometallic cation on a polyvacant heteropolytungstate.[18] This strategy which consists in matching the reactivity and geometry of the complementary moieties was found to be particularly convenient for the synthesis of multi-unit nanosized clusters.[19] The dinuclear oxo–thio cations $[M_2O_2S_2]^{2+}$ (M = Mo or W), one of the aforementioned structural archetypes[20] were reacted as electrophiles with divacant[18,21] or trivacant nucleophilic polyanions[22] to give highly stable assemblies. Müller *et al.* successfully transposed this convenient procedure to the reaction of monovacant polyanions toward the pseudocuboidal fragment $[Mo_3S_4]^{4+}$.[23]

These first results were at the origin of our ideas about the possibilities of preparing large sized (oxo)thiocompounds by self-condensation of the $[M_2O_2S_2]^{2+}$ fragment. In fact, we have developed an approach comparable to that commonly employed in POM chemistry.[24] Even if the coordination properties of $[M_2O_2S_2]^{2+}$ have been extensively investigated,[25,26] curiously nothing has been reported on the acido–basic properties and the resulting polycondensation abilities of this fragment. The double sulfido bridge confers to the $[M_2O_2S_2]^{2+}$ building block specific coordination properties, at the origin of a unique class of compounds, not observed with the full oxo analogue $[Mo_2O_4]^{2+}$.[27,28] Cyclic architecture is the common feature of this family of compounds giving rise to supramolecular properties potentially relevant to anion recognition, anion-templated synthesis and 3-D structures. Some examples of host–guest implications are presented relating to both the solid state and solutions. Molecular dynamic and exchange properties are also discussed. We first present the basic concepts of this chemistry, which are key for the development of *'the building block approach'* for constructing large oxothiometallic cyclic molecules. Hence, this article illustrates how the self-condensation of the $[M_2O_2S_2]$ fragment represents a reliable and rational method to prepare original cyclic oxothio compounds.

Emmanuel Cadot was born Paris in 1963. He obtained his first degree at the University Pierre et Marie Curie in 1988 and received a Ph. D. degree from the same University in 1991. After working one year at the Institut de Recherche sur la Catalyse in Lyon (France) as a postdoctoral fellow, he moved to Versailles, joining Sécheresse's group in 1993 where he achieved his current position as Assistant Professor in the Department of Chemistry of the University of Versailles St-Quentin. He recently received his habilitation to direct researches. His interest focusses on the synthesis and assembly of mixed polyoxothiometallates.

Francis Sécheresse is a graduate of the University Pierre et Marie Curie. He received his Ph. D. degree in 1973 and prepared his thesis under the supervision of Professor J. Lefèbvre in the Laboratory of Professor P. Souchay. In 1986, he joined the laboratory of Professor Y. Jeannin as Assistant Professor. In 1992, he was appointed Professor of Chemistry at the University of Versailles St-Quentin. His research interests include polyoxo(polythio) metalate chemistry, inorganic materials chemistry, polycondensation processes and reactivity.

DOI: 10.1039/b203497m

Basic concept

Generally, the formation of polyoxometallates results from the acidification of a solution containing the basic monomeric oxoanions $[MO_4]^{2-}$ (M = Mo or W).[24] The presence of small anionic assembling groups with fixed geometry, for instance tetrahedral (phosphate or silicate) or trigonal (arsenite or antimonate), directs the aggregation process providing numerous oxygen–metal cluster anions.[29] We envisaged to transpose this convenient approach to a sulfur-containing precursor. Obviously, the first goal was the choice of the ionic precursor which has to exhibit a good stability during the aggregation process, with an adapted electronic structure and adequate coordination requirements to form well-defined discrete polyoxothiometalates. According to our experience on Mo(W)–S chemistry, the $[Mo_2O_2S_2]^{2+}$ dication was chosen as starting 'monomer'. The overall geometry of the dication is shown in Fig. 1. The two Mo^{5+} centers are equivalent and are linked by a

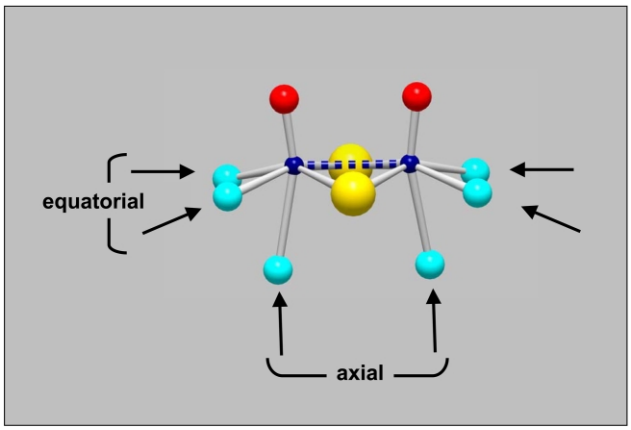

Fig. 1 Primary building unit $[Mo_2S_2O_2(H_2O)_6]^{2+}$ (O, red; S, yellow, Mo, dark blue; aquo ligand, light blue).

double sulfido bridge. A metal–metal bond [$d(Mo^V \cdots Mo^V)$ ~ 2.8 Å] participates to the cohesion of the unit and confers an excellent stability to the cation, even in strongly acidic medium.[30] Each Mo atom is also bonded to one terminal oxygen atom. In aqueous medium, the coordination sphere of each molybdenum atom is achieved by three water molecules resulting in the aqua ion $[(H_2O)_6Mo_2O_2S_2]^{2+}$.[30,31] These coordination water molecules are polarized enough to be ionized and establish inter-building block connections *via* a Mo–OH–Mo bonding scheme. Finally, the aggregation process is revealed to be sensitive to the presence of specific structuring agents. The analogy between the formation of polyoxometallates from oxoanions and that of polyoxothioanions from oxothiocations is exemplified in Scheme 1.

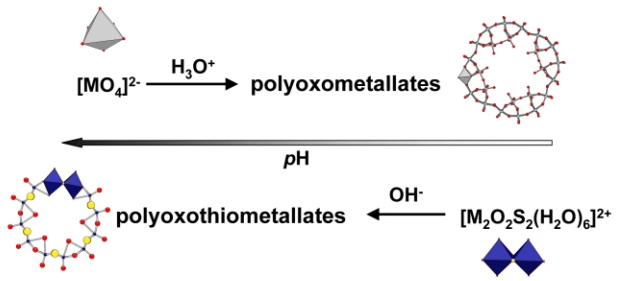

Scheme 1

Formation of the dication

We have adopted the procedure described by Coucouvanis, who showed that the selective oxidation of the terminal $(S_n)^{2-}$ groups by iodine in $[(S_2)MoOS_2MoO(S_4)]^{2-}$ quantitatively led to the $[Mo_2O_2S_2]^{2+}$ cation.[32] This protocol, initially described for DMF medium, was successfully adapted by us for aqueous medium, using the $[(S_2)MoOS_2MoO(S_2)]^{2-}$ anion as its tetramethylammonium salt (Scheme 2).[33] The facile synthetic

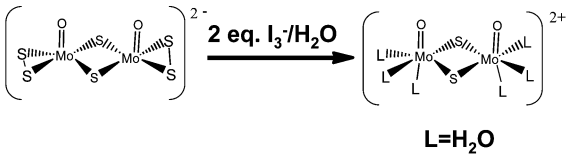

Scheme 2

procedure of the former dianion described by Müller *et al.* allows the sulfur containing precursor to be obtained in high yield.[34] The use of water as solvent is really the key point since it permits control of the condensation process, formally deriving from an olation reaction,[35] by simple pH measurements.

From the building block to polynuclear rings

(i) The first elements of the series

A yellow microcrystalline powder precipitated by direct addition of potassium hydroxide to a mixture of the dithiocation and potassium iodide until pH 2–3. The composition of the solid **1** indicates the presence of iodide ions with potassium cations as counter ions. After crystallisation in *pure* water, **1** gave the iodide-free neutral dodecameric wheel, $[Mo_{12}O_{12}S_{12}(OH)_{12}(H_2O)_6]$ **2** while in DMF containing tetrabutylammonium halides, the bis-halide decameric wheels $[X_2Mo_{10}O_{10}S_{10}(OH)_{10}(H_2O)_5]^{2-}$ (X = Cl, **3b** or I, **3a**) were obtained.

Mo_{12}-ring (2). The structural characterization of **2** reveals a discrete dodecameric ring made up of six $\{Mo_2O_2S_2\}$ fragments, linearly connected by double hydroxo bridges (Fig. 2).[36]

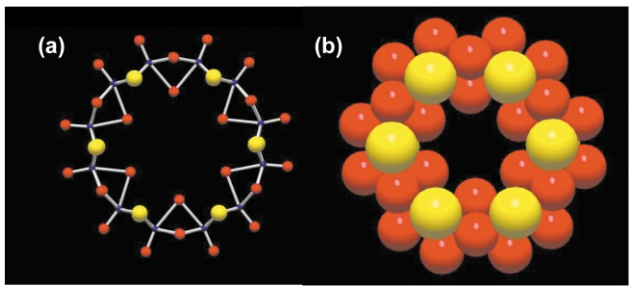

Fig. 2 Views of the $[Mo_{12}S_{12}O_{12}(OH)_{12}(H_2O)_6]$ ring cluster: (a) ball-and-stick model; (b) space-filling representation (S^{2-}, 1.82 Å; O^{2-}, 1.40 Å; Mo^{5+}, 0.55 Å).

The cyclic backbone $\{Mo_{12}O_{12}S_{12}(OH)_{12}\}$ is neutral and delimits a central open cavity of about 11 Å, lined by six water molecules. These aquo ligands are bound to two adjacent molybdenum atoms conferring an unusual pseudo-sp^3 hydridization to the water oxygen atom. Such a molecule can be viewed as an "inverse crown ether" like-compound. The inner water molecules are labile enough to be exchanged for specific anions, suggesting the cavity exhibits a cationic character, induced by the presence of twelve Mo^{5+}. This situation contrasts with that encountered with conventional crown ether compounds where the cavity is lined by donor oxygen atoms giving the cavity an anionic character. In this sense, the "inverse" designation correctly describes this inorganic macrocycle. The beauty of this structure lies in the high symmetry of the architecture (D_{6h}) and the simplicity of the coordination path ensuring the inter-block connections. Only the four equatorial aquo ligands of the initial dithiocation are involved in the olation reaction (see Fig.

1). Such results evidence the difference of reactivity between the two types of potential sites of polycondensation, *i.e* axial and equatorial. The four equatorial aquo ligands are ionized below pH 2, initiating the oligomerization process, while the two axial water molecules remain unaffected in the neutral Mo_{12}-ring. Their ionization successively occurs in a distinct pH domain, between 4.5 and 9 (see below). The acido–basic properties, coupled with the poor reactivity of the bridging sulfur atoms in the synthesis conditions are the main reasons, but likely not the only ones, that constrain the mode of connection to be linear.

Mo_{10}-ring (3). The crystallization of **1** in DMF containing tetrabutylammonium iodide[37] or tetraethylammonium chloride[38] leads to the compounds $(TAA)_2[X_2Mo_{10}S_{10}O_{10}(OH)_{10}(H_2O)_5]$ with TAA = NBu_4 and X = I or TAA = NEt_4 and X = Br, respectively. Both the $[X_2Mo_{10}]^{2-}$ (**3a** for X = I and **3b** for X = Cl) molecular structures are similar, revealing a neutral decanuclear ring (Fig. 3), which

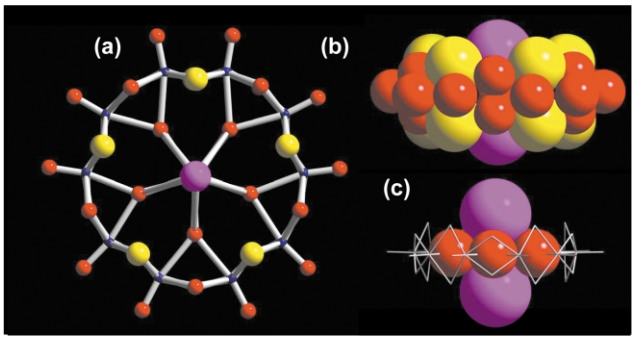

Fig. 3 Molecular structure of $[I_2Mo_{10}S_{10}O_{10}(OH)_{10}(H_2O)_5]^{2-}$ **3a**: (a) ball-and-stick model; (b) space-filling side view (I^-, 2.2 Å) showing the two iodide ions fitting on both sides of the open cavity and (c) forming a close-compact inner cluster $\{(H_2O)_5I_2\}^{2-}$.

exhibits exactly the same connection pathway as the previously described Mo_{12}-ring. In the solid state, the neutral decameric ring is associated with two halide ions. The two halides are symmetrically located on both sides of the mean plane defined by the ten Mo atoms. This observation is not only a solid state peculiarity since the two halides ions interpenetrate the cavity of the cycle to form a genuine supramolecular bis-halide complex (Fig. 3(b)). The distances between the two halides and the five oxygens atom of the ring are short enough to suggest that the stability of the supramolecular arrangement is directly related to the existence of a H-bonding network involving the protons of the inner water molecule. Two groups of five hydrogen bonds symmetrically converge toward the central halides and cause a pronounced shortening of the X···X distances (see Table 1), to

Table 1 Selected distances in the $\{X_2(H_2O)_5\}^{2-}$ central core

Distance/Å	X = Cl^-	X = I^-
O···X^-	3.28 (3.21)[a]	3.61 (3.60)[a]
X^-···X^-	3.82 (3.62)[a]	4.78 (4.40)[a]

[a] Calculated values for a close packed model from ionic radii with 1.81 Å for Cl^-, 2.20 Å for I^- and 1.40 Å for O^{2-}

rather close to the sum of their ionic radii. As depicted in Fig. 3(c), the $\{(H_2O)_5X_2\}^{2-}$ central core exhibits a quite close compact arrangement.

Mo_{10}–Mo_{12} relationship. Mo_{12} and Mo_{10} are obtained through a 'soft' process of recrystallization starting from the same solid **1**. Although the structure of this microcrystalline powder has not been established, the elemental analysis of **1** is consistent with a molecular formula $[I_2Mo_{10}S_{10}O_{10}(OH)_{10}(H_2O)_5]^{2-}$ for the anion, and as a working assumption, we propose a rational interconversion process between Mo_{12} and Mo_{10} rings. In water, successive equilibria based on halide exchanges can be reasonably suggested, which formally lead to the iodide free neutral cluster [eqns. (1) and (2)]. Clearly, the neutral decamer self-rearranges to yield the neutral dodecamer [eqn. (3)]. In contrast, the self-rearrangement

$$[I_2Mo_{10}]^{2-} \rightleftarrows [IMo_{10}]^- + I^- \quad (1)$$

$$[IMo_{10}]^- \rightleftarrows [Mo_{10}] + I^- \quad (2)$$

$$1.2\ [Mo_{10}] \rightleftarrows [Mo_{12}] \quad (3)$$

of the ring is locked in halide concentrated DMF solution, which suggests that the presence of halide ions (Cl^- or I^-) and/or aprotic solvent contribute to maintain the Mo_{10} backbone. Further investigations in aqueous solution confirmed that only the presence of halide ions is necessary to maintain the Mo_{10} nuclearity. We have studied the acido–basic properties of the Mo_{10} ring in aqueous solution containing chloride ions. Potentiometric titration curves agree with successive ionization of the five inner water molecules in the neutral $[Mo_{10}]^0$ leading to the ionized $[Mo_{10}]^{5-}$ polyanion. The five related acidity constants vary smoothly from 4 to 9. At pH 6–6.5 we isolated and crystallographically characterized the $[Mo_{10}]^{2-}$ anion as a monohalide complex $[ClMo_{10}O_{10}S_{10}(OH)_{12}(H_2O)_5]^{3-}$ **4**. The molecular structure resembles the neutral analogue but on replacing two inner aquo ligands by hydroxo groups, the inorganic cycle interacts with only a single chloride. The two removed protons are replaced by lone pairs as illustrated in Fig. 4, which induced unfavorable interactions towards a second halide ion.

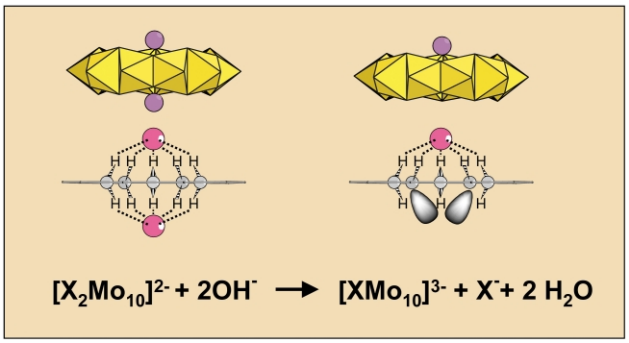

Fig. 4 Schematic representation of the influence of the ionization process for change from a bis-halide to a mono-halide cluster.

From this point of view, the halide ions can be viewed as templates for dictating the nuclearity of the wheel, which can swing from ten to twelve. Hence, the ability of the cyclic rings to self-rearrange, supported by the 'sensitivity' of such systems toward 'soft' bases such as halides open some interesting perspectives in the field of templated-synthesis and host–guest chemistry.

(ii) Templated synthesis with carboxylate ions

The previous results prompted us to wonder if we could extend to a further stage a cycle-based chemistry by synthesizing derived rings of different shapes and sizes? Regarding the basic mode of connection between the primary building blocks in **2** and **3**, the possibility to tune the size and shape of the ring by using a suitable template in the condensation process seemed an obvious opportunity. Hence, our attention focussed on the reactivity of the cavity of the ring, switching to 'stronger' bases such as carboxylate ions to substitute the inner water molecules. The use of linear dicarboxylates, oxalate ($C_2O_4^{2-}$), glutarate ($H_6C_5O_4^{2-}$) and pimelate ($H_{10}C_7O_4^{2-}$) ions proved to be excellent examples to study the influence of the length of the alkyl chain on the size of the wheel. The presence of oxalate,

glutarate and pimelate ions in the synthesis medium give specifically $[Mo_8S_8O_8(OH)_8(C_2O_4)]^{2-}$ ($[Mo_8\text{-ox}]^{2-}$), $[Mo_{10}S_{10}O_{10}(OH)_{10}(H_6C_5O_4)]^{2-}$ ($[Mo_{10}\text{-glu}]^{2-}$) and $[Mo_{12}S_{12}O_{12}(OH)_{12}(H_{10}C_7O_4)]^{2-}$ ($[Mo_{12}\text{-pim}]^{2-}$) anions.[39] This series of compounds, $[Mo_8\text{-ox}]^{2-}$ **5**, $[Mo_{10}\text{-glu}]^{2-}$ **6** and $[Mo_{12}\text{-pim}]^{2-}$ **7**, were structurally characterized and clearly demonstrated that it is possible to vary the size of the ring in a very simple way. Their molecular architectures, given in Fig. 5,

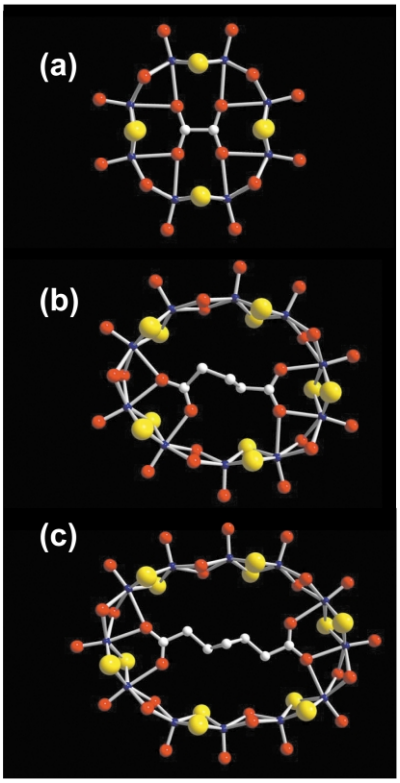

Fig. 5 Encapsulated dicarboxylate ions: molecular view of (a) $[Mo_8S_8O_8(OH)_8(C_2O_4)]^{2-}$ **5**, (b) $[Mo_{10}S_{10}O_{10}(OH)_{10}(H_6C_5O_4)]^{2-}$ **6** and (c) $[Mo_{12}S_{12}O_{12}(OH)_{12}(H_{10}C_7O_4)]^{2-}$ **7**.

consist of a neutral inorganic ring $\{Mo_{2n}O_{2n}S_{2n}(OH)_{2n}\}$, n = 4, 5 or 6 for ox^{2-}, glu^{2-} or pim^{2-}, respectively, encapsulating the guest linear dicarboxylate ion. The cyclic skeleton of **5** contains eight octahedral molybdenum atoms that closely confines the central oxalate anion. Each oxygen atom of the two equivalent carboxylate groups is doubly bonded to two adjacent Mo atoms. The structures of $[Mo_{10}\text{-glu}]^{2-}$ **6** and $[Mo_{12}\text{-pim}]^{2-}$ **7** formally derive from those of their symmetrically circular Mo_{10} **3** and Mo_{12} **2** parents, respectively, but appear severely puckered by the presence of the guest anion. The encapsulated dicarboxylate groups directly coordinate the Mo atoms at opposite ends of the ring. Likely due to steric constrains induced by the central alkyl chain, no inner water molecules were found in the cavities of **6** and **7**, which reveal that the Mo atom is able to adopt either an octahedral or square pyramidal coordination. This possibility for the Mo^V centers to be six- or five-fold coordinated leads to a great flexibility in these architectures. Indeed, the Mo–Mo–Mo angles can vary from 135 to 180° in a given structure, while the interblock connections can be face- or edge-sharing. Acting as 'pincers' at the opposite sides of the ring, the caboxylate groups reduce related Mo–Mo–Mo angles. The cycle flattens to adapt the geometry of the cavity to that of the encapsulated molecule. Aqueous solution ^{1}H NMR studies of **6** and **7** evidenced the encapsulated organic moiety, which exhibits systematically shielded ^{1}H chemical shifts, while electrospray mass spectrometry investigations on aqueous solution of **5**, **6** and **7** indicate that the corresponding crystal structures are maintained in solution.

The last and pleasing example of a ring template effect concerns the trimesate ion (1,3,5-methylcarboxylatobenzene) which generates anion **8**, a perfectly circular Mo_{12} dodecameric ring.[40] The encapsulated trimesate lies in the mean plane defined by the twelve molybdenum atoms, locked into this position by the three anchoring carboxylato groups. Thus, the ring ideally fits with the guest, resulting in the circular outline shown in Fig. 6. At this stage, numerous clear perspectives can

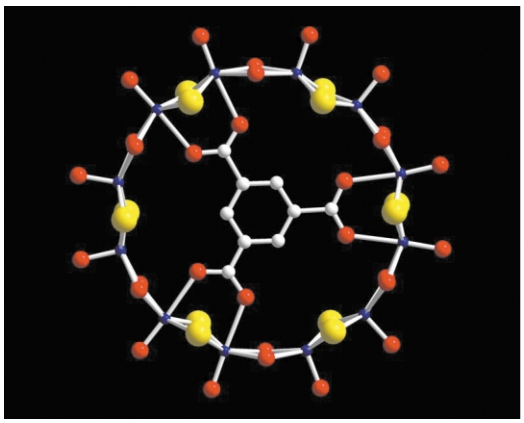

Fig. 6 An example of a perfectly adapted host–guest symmetry: $[Mo_{12}S_{12}O_{12}(OH)_{12}(H_3C_9O_6)]^{3-}$ **8**.

be predicted for the synthesis of hybrid inorganic–organic molecular materials with regard to the multi-functionality, conformation and design, size and shape, deriving from organic polycarboxylic acids.

'Wheeling template'. The extreme flexibility of these rings led us to investigate the dynamics of the host–guest interactions in $[Mo_8\text{-ox}]^{2-}$ **5**, $[Mo_{10}\text{-glu}]^{2-}$ **6** and $[Mo_{12}\text{-pim}]^{2-}$ **7**, which was studied by ^{1}H NMR spectroscopy from CD_3CN solutions at various temperatures in the range 320–226 K. The resulting ^{1}H NMR spectra of $[Mo_{10}\text{-glu}]^{2-}$ **6** solutions are shown in Fig. 7.

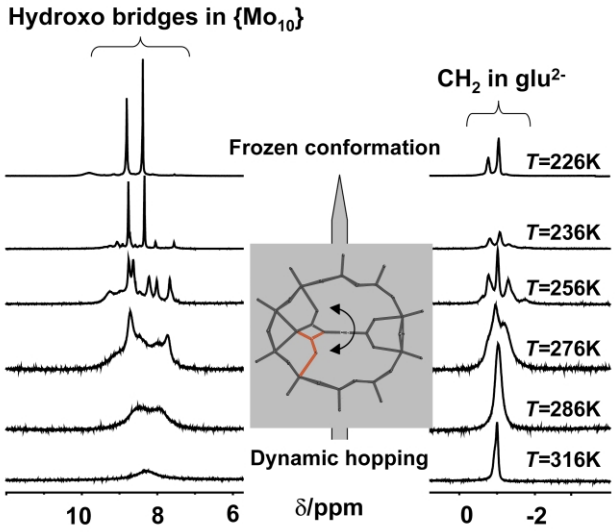

Fig. 7 Variable-temperature ^{1}H NMR spectra of $[Mo_{10}\text{-glu}]^{2-}$ **6** in CD_3CN with evidence of a dynamic shuttle of the central guest.

The pronounced evolution with temperature of the ^{1}H NMR spectra, in the region related to the inorganic hydroxo bridges constituting the wheel (8–10 ppm),[41] as well as in the region corresponding to the CH_2 groups of the central alkyl chain (~ -1 ppm) are directly related to the fluxionality of the host–guest systems. At room temperature, the central glutarate randomly wheels in the cavity, owing to the concerted hopping of the two terminal carboxylate groups over the ten molybdenum atoms. Such a dynamics is strongly facilitated by the

versatility of the Mo^V coordination which can be either octahedral or square pyramidal. Thus, the motions of the guest in the host ring result from a dynamical synergy based on the flexibility of the molecular framework: the hopping of a carboxylate group from a Mo atom to the closest one causes deformations in the wheel and reciprocally, deformations in the wheel induce the internal rotation of the carboxylate fragment. At low temperature (226 K), this dynamic process is very slow on the NMR time scale, so giving a unique frozen host–guest conformation. The ^{1}H NMR spectrum of the $[Mo_{12}\text{-pim}]^{2-}$ **7** anion exhibits a comparable temperature-dependence (not shown), essentially interpreted in the same way. ^{1}H NMR spectra of $[Mo_8\text{-ox}]^{2-}$ **5** contrast with this situation since no temperature dependence is observed. In this case, the oxalate ion ensures a stronger rigidity to the inorganic backbone in which all the Mo atoms have an octahedral environment. Such an arrangement prevents any concerted internal rotation of the two central carboxylate groups.

1-D supramolecular chain. In the presence of a slight excess of glutarate ion, the $[Mo_{10}\text{-glu}]^{2-}$ ring **6** interacts with an additional glutarate ion leading to the supramolecular arrangement $\{glu\text{-}[Mo_{10}\text{-glu}]\}^{4-}$ **9** depicted in Fig. 8. Both the

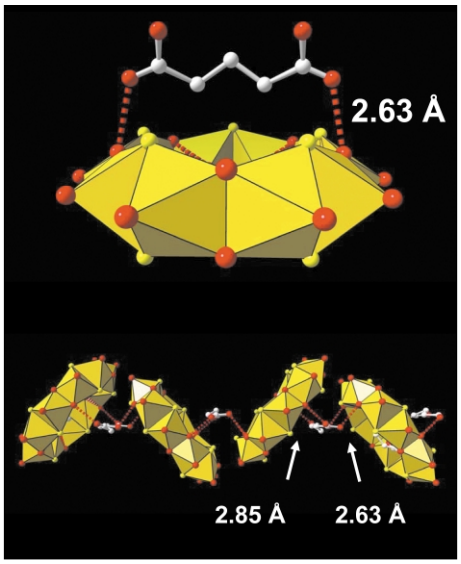

Fig. 8 Hydrogen-bonding pattern between $[Mo_{10}\text{-glu}]^{2-}$ **6** and outer glutarate in the solid state to give $\{(H_6C_5O_4)[Mo_{10}S_{10}O_{10}(OH)_{10}(H_6C_5O_4)]\}^{2-}$ **9**: ″basket-handle″ supramolecular association (top) and resulting zigzag chain with alternance of short and long O···O distances (bottom).

carboxylate groups of the outer glu^{2-} ion are connected to the cycle through H-bonds involving two bridging hydroxo groups of the Mo_{10} ring (O···O distances of 2.63 Å). The resulting basket-handle associations are mutually connected through a second set of H-bonds (O···O distances of 2.85 Å) to produce infinite zigzag chains.

Extension to tungsten. The breakthrough in our search for preparing larger templated rings came unexpectedly when we turned our efforts to the polycondensation products of the $[W_2O_2S_2]^{2+}$ tungsten analogue. Here, attempts to prepare a concentrated solution of the $[W_2O_2S_2]^{2+}$ dithiocation by analogy with molybdenum are hampered by serious problems of stability: the $[W_2O_2S_2]^{2+}$ dithiocation slowly decomposes in acidic aqueous medium with H_2S evolution into insoluble unidentified products. These difficulties can be successfully avoided by the use of an aprotic coordinating solvent such as DMF.[42] The second stage consisting of the polycondensation process of the primary dication is monitored in mixed aqueous–DMF medium, while the final products are crystallized in pure water. Further investigations have proved that the polyoxothiotungstate architectures are indefinitely stable in aqueous medium, the stability enhancement mainly depending on the charge changing from cationic to neutral or anionic. Then, the self-condensation of the $[W_2O_2S_2]^{2+}$ building block, in the presence of glutarate ion, effects a spectacular ring expansion in the form of the unprecedented sixteen-metal macrocycle $[W_{16}O_{16}S_{16}(OH)_{16}(H_2O)_4(H_6C_5O_4)_2]^{4-}$ **10** ($[W_{16}\text{-glu}_2]^{4-}$).[43] Our surprise was not restricted to the exceptional size of the ring but was increased by the evidence in the solid state of two frozen conformations, **10a** and **10b**. The composition of the solids containing **10a** and **10b** are quite similar, differing only by one molecule of crystallization water among thirty three located in the crystal packing, while the molecular backbones exhibit exactly the same composition. Fig. 9 shows the

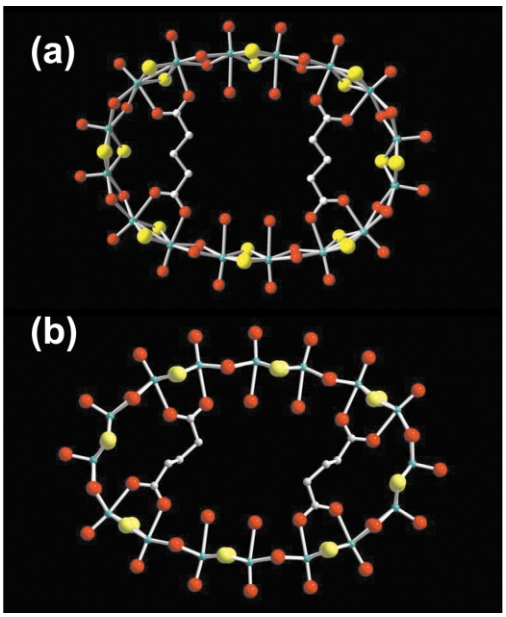

Fig. 9 Two conformers of the molecular structure of $[W_{16}O_{16}S_{16}(OH)_{16}(H_2O)_4(H_6C_5O_4)]^{4-}$: (a) highly symmetric D_{2h} form **10a** in the orthorhombic phase; (b) distorted C_2 form **10b** in the monoclinic phase.

molecular architectures of **10a** and **10b**. The connection pathway between the building blocks remains unchanged with respect to those observed in analogous Mo rings. Here, the $\{W_{16}O_{16}S_{16}(OH)_{16}\}$ ring system acts as a macrocyclic host including two glutarate ions, which are symmetrically arranged as flexible pillars in the open cavity. Four inner water molecules are located within the cycle, each being bonded to a tungsten atom through a long W–OH_2 bond (2.40 Å). Steric constraints in the cavity impose a square pyramidal environment for four tungsten atoms. Compounds **10a** and **10b** differ in their crystal packing, (othorhombic for **10a** and monoclinic for **10b**), the symmetry of the wheel being also slightly but significantly affected. In the orthorhombic system, the wheel adopts the more symmetric conformation (D_{2h}) while in the monoclinic form, the symmetry is lowered to C_2. The two structures are related by weak deformations, which can be described as antiparallel stretches. Such results illustrate and support our previous conclusions about the high flexibility of these systems. Here, these two conformations can be viewed as two snapshots of the dynamic scenario occurring in solution.

The nuclearity of the cycle depends on steric strains imposed by the template and hence the number of template moieties within the ring is an additional and critical parameter. The specificity of the reaction for a deliberate ring-shape or size should essentially depend on the synthesis conditions such as temperature, concentration, solvent, *etc*. In this regard, the exact conditions, which permit the deliberate synthesis of a mono-templated ring as $[Mo_{10}\text{-glu}]^{2-}$ **6** or a bis-templated ring as $[W_{16}\text{-glu}_2]^{4-}$ **10**, are not yet completely understood and studies are in hand to find answers to this crucial question.

(iii) Phosphate exchange in molecular rings

We also turned our efforts on phosphate anions acting as ring-templating agents, owing to their chelating properties, small size and tetrahedral geometry. We succeeded in isolating and characterizing mono- and di-phosphato rings, **11** and **12**, respectively.[44] The structure of **11** depicted in Fig. 10 reveals a

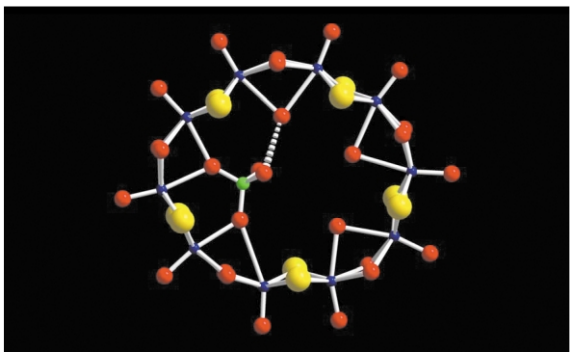

Fig. 10 Molecular view of the monophosphato $[(HPO_4)Mo_{10}S_{10}O_{10}(OH)_{10}(H_2O)_3]^{2-}$ **11** anion.

decanuclear ring $\{Mo_{10}O_{10}S_{10}(OH)_{10}\}$ encapsulating a single hydrogenphosphate $[HPO_4]^{2-}$ anion. Crystals of such an assembly were grown from nearly stoichiometric phosphate from dilute aqueous solutions. Increasing the phosphate content, or operating in more concentrated solutions switches the system toward the diphosphato ring **12**, shown in Fig. 11. The

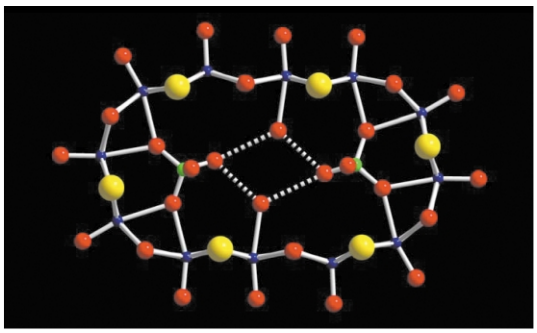

Fig. 11 Molecular view of the diphosphato $[(HPO_4)_2Mo_{12}S_{12}O_{12}(OH)_{12}(H_2O)_2]^{4-}$ **12** anion.

twelve-metal ring in **12** is shown to encapsulate two hydrogenphosphate groups $[HPO_4]^{2-}$. Because of the chelating effect of the two hydrogenphosphate groups, the Mo_{12}-ring is strongly distorted from circular to elliptical. Here, the severe flattening of the ring shape is attributed to both electrostatic repulsions between the diametrically opposed hydrogenphosphate groups and to their coordination pincer effects. The cohesion of the elliptical shape is supported by the existence of internal hydrogen bonds involving the deprotonated P=O bonds and terminal inner water molecules (Fig. 11). Variable-concentration experiments allowed us to identify and attribute the ^{31}P NMR resonances of the two hydrogenphosphate-containing rings, $[PMo_{10}]^{2-}$ and $[P_2Mo_{12}]^{4-}$, present in solutions and establish the thermodynamical equilibrium that connects them (eqn. (4)).

$$[P_2Mo_{12}]^{4-} \rightleftarrows 1.2\ [PMo_{10}]^{2-} + 0.8\ [P]^{2-} \qquad (4)$$

An additional and striking point is raised by variable-temperature and phosphate–arsenate exchange experiments. As already observed with dicarboxylate ions, the hydrogenphosphate groups tumble into the cavity, hopping on the vacant adjacent coordination sites. Further, fast dynamical exchanges take place involving uncoordinated and coordinated hydrogenphosphate ions in the Mo_{10} and Mo_{12} ring systems. Interestingly, the hydrogenphosphate-containing ring systems perfectly illustrates our previous observations on the relationship between ring expansion and the number of encapsulated template-agents. A single hydrogenphosphate stabilizes a ten-metal ring, while the insertion of the second causes ring expansion to a twelve-metal cyclic architecture. As a consequence of eqn. (4), an increase of the phosphate content in solution changes the $[P_2Mo_{12}]:[PMo_{10}]$ (**12**:**11**) ratio. Thermodynamic equilibrium is instantaneously reached, highlighting the extreme versatility of the $\{Mo_{2n}S_{2n}O_{2n}(OH)_{2n}\}$ ring skeleton in aqueous solution, through dynamic breaking and formation of interblock connections. Beyond a phosphate concentration of 0.5 mol L^{-1} the expected ring expansion is no longer observed and the polycondensation process turns the system toward another topology.

In concentrated phosphate solutions, the self-condensation of the dithiocation produces exclusively the hexameric $[(HPO_4)_4Mo_6S_6O_6(OH)_3]^{5-}$ anion **13**, characterized in solution by ^{31}P NMR spectra and in the solid state by crystallography.[45] In this compound, the building blocks connections are ensured through a single shared hydroxo group and a bridged peripheral hydrogenphosphate. The six-metal ring surrounds a central hydrogenphosphate to finally give a quite close compact arrangement of oxo and sulfur ions (Fig. 12). In the course of

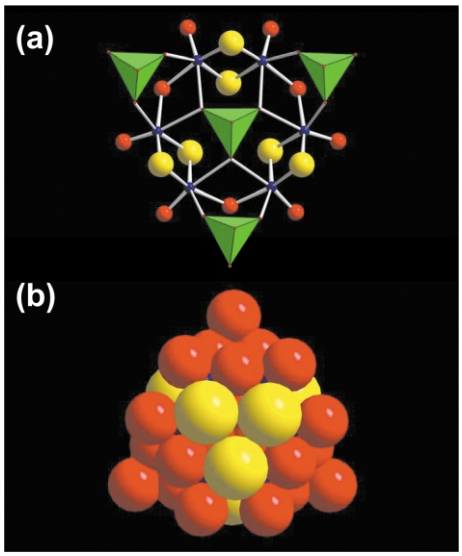

Fig. 12 Representations of $[(HPO_4)_4Mo_6S_6O_6(OH)_3]^{5-}$ **15**.

this study, the arsenato derivative $[(HAsO_4)_4Mo_6S_6O_6(OH)_3]^{5-}$ **14** was also structurally characterized.[45] Further investigations in solution reveal two kinds of reactivity for compound **13**. (i) The first concerns the three peripheral hydrogenphosphates, which are shown to be labile enough to be replaced by other functional groups. For modeling the substitution reaction, we have studied hydrogenphosphate replacement by acetate groups. According to ^{31}P NMR spectroscopy, the exchange was found to be successive, leading to the formation of mixed acetato–phosphato species. We found through quantitative treatment of the data, that the relative affinity of both the substituting groups toward the coordination sites are essentially related to their acidity constants. (ii) The other reaction mode corresponds to the selective replacement of sulfur atoms within the $\{Mo_2S_2O_2\}$ fragment through nucleophilic attack of hydroxide ions.[46] The latter reaction takes place under more drastic conditions (80–100 °C) and in agreement with ^{31}P NMR studies, the nucleophilic substitution appears to be regioselective. In the first step, the substitution process relates only to the three sulfur atoms in the same plane, located at the opposite side of the four hydrogenphosphate groups. The other three sulfur atoms seem to be protected by the four bulky hydrogenphosphates located nearby. We succeeded in isolating the half-desulfurated $[(HPO_4)_4Mo_6S_3O_9(OH)_3]^{5-}$ anion **15**,[46] the

crystallographic structure of which unambiguously supports our previous ^{31}P NMR observations in solution.

This arrangement, $\{P_4Mo_6\}$, can be viewed as an hexavacant anion derived from the ε Baker–Figgis isomer[47] of the Keggin cluster[48] known for a long time in aluminium polycations[49] and recently isolated as a polyoxomolybdate.[50,51] In this regard, the apparent analogy of this system with heteropolyxometalate chemistry convinced us of the potentialities of the $[M_2S_2O_2]$ synthon to generate a wide diversity of compounds, structurally based on the geometry of the primary basic building block. Besides, the final properties of these species can be tuned by the replacement of (hydrogen)phosphates for specific functional groups, giving the chemist real possibilities for structural extensions in the field of inorganic supramolecular chemistry.

(iv) Mixed-metal rings

We have seen that organic and p-block oxo-anions could be used as ring template agents. However, more sophisticated species such as transition-metal based templates have been also used as structuring or directing agent. Under stoichiometric conditions of $[MO_4]^{2-}$ (M = Mo or W) tetraoxometalate ions, the self-condensation of the $[Mo_2O_2S_2]^{2+}$ precursor yields the mixed-metal $[Mo_8S_8O_8(OH)_8\{HMO_5(H_2O)\}]^{3-}$ anions **16** (M = Mo) and **17** (M = W).[52,53] The molecular structures of the two compounds were determined by X-ray diffraction study and are similar (Fig. 13). They consist of an octameric ring

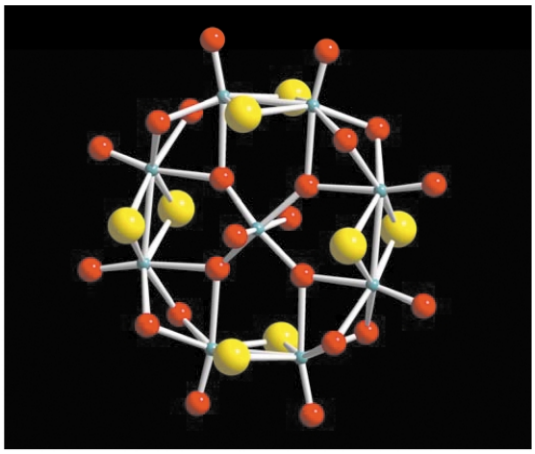

Fig. 13 Ball-and-stick representation of $[Mo_8S_8O_8(OH)_8(H_3MO_6)]^{3-}$ (M = Mo **16** or W **17**).

$\{Mo_8S_8O_8(OH)_8\}$ that encapsulates a central $\{M^{VI}O_6\}$ octahedron. For comparison, this arrangement is quite similar to that previously described with oxalate ion, see Fig. 5(a). The four equatorial oxygen atoms attached to the central metal center are triply bonded and equally shared with two adjacent Mo^V atoms. The central metal atom is significantly displaced out of the mean plane defined by the eight Mo atoms to give a short M=O and a longer M–OH_2 bond. It should be noted that the geometry of the encapsulated species has changed from tetrahedral to octahedral to give a central mononuclear formally anionic $\{H_3MO_6\}^{3-}$ (M = Mo or W), stabilized by the surrounding Mo_8-ring. Although anion **16** contains a mixed-valence Mo^{VI}/Mo^V system, its electronic spectrum does not exhibit any intervalence charge transfer (IVCT) from peripheral Mo^V atoms toward the central Mo^{VI}, but appears to be mainly dominated by E→M (E = O, S) charge transfer transitions from the ligands to the metal centers. The eight electrons are firmly trapped as pairs in bonding molecular orbitals mainly localized within each building block (Mo–Mo bonds), and in addition the connectivities between the Mo^V and Mo^{VI} centers are ensured through long Mo–O bonds (2.2–2.4 Å) in *trans* positions to the Mo=O double bonds. Thus, such compounds exhibit strongly trapped mixed valence (class I in the Robin and Day classification). The formation of the tungsten analogue $[W_8S_8O_8(OH)_8(H_3WO_5)]^{3-}$ **18** was observed for stoichiometric ratios of $[W_2O_2S_2]^{2+}$ and $[WO_4]^{2-}$ in self-condensation conditions at pH = 5.[54] Anion **18** displays an electronic spectrum similar to that for **16**. The mixed-metal ring system could represent a promising method for increasing the complexity level of elaborated materials. One can easily envisage that rings could encapsulate even more sophisticated anions, for instance derived from the well-known POMs.

Extended structures with cyclic oxothiometalates

Among the molecular structures previously described, some give rise to beautiful Platonic networks meriting brief discussion here.[55] Ionic packing generally results from direct connections between oxo or hydroxo groups of the rings and alkali cations, commonly Li^+, Na^+ or K^+. The networks can be formally regarded as resulting from a two-stage process, beginning by the formation of a sub-cationic framework, acting as scaffolds on which the anionic rings are connected. The charge and shape of the molecular rings, as well as the nature and variable coordination of the alkali ions can lead to multiple combinations for anion–cation connections which explain the unpredictable nature of this area.

Cationic pillars

The elliptical diphosphato ring **12** crystallizes as the sodium salt Na_4**12**·$27H_2O$. A representative view of the solid is shown in Fig. 14. The Na^+ cations are mutually connected through edge-

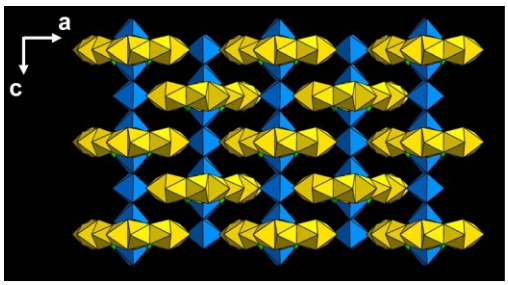

Fig. 14 3-D arrangement in $Na_4[(HPO_4)_2Mo_{12}S_{12}O_{12}(OH)_{12}(H_2O)_2]\cdot 27H_2O$, Na_4**12**·$27H_2O$, showing the Na^+ pillars along the *c* axis.

sharing octahedra to form parallel pillars running along the *c* axis. The cyclic polyanions are perpendicularly stacked along these linear columns so ensuring the cohesion of the array. In a similar way, the mixed-metal octameric ring $[H_3Mo_8WS_8(OH)_8O_{14}]^{3-}$ **17**, as its lithium salt in Li_3**17**·$18H_2O$, see Fig. 15, leads to a comparable network. However, the Li^+ cations adopt alternately octahedral and tetrahedral coordination and are mutually connected through edge shared polyhedra. The junctions between Li^+ pillars and rings form planes which stack along the *b* direction. The large voids resulting from these connections are filled by large disordered clusters $(H_2O)_{10}$, structurally characterized by neutron diffraction. Ionic conductivity measurements were performed on pressed pellets and single crystals revealing excellent conductivity (2.2×10^{-5} S cm^{-1}), a value slightly smaller than that observed for the best crystalline protonic or lithium conductors.[56]

Cationic planes

The supramolecular arrangement of the mono-chloride complex $[ClMo_{10}S_{10}O_{10}(OH)_{12}(H_2O)_3]^{3-}$ **4** crystallizes as potassium salt in K_3**4**·$14H_2O$. K^+ polyhedra form planes parallel to (010), which delimits ten potassium ring domains, exactly filled by a first set of **4**, (Fig. 16(a)). These planes are connected through a second set of **4** to produce a notable 3-D array. The resulting grid delimits large ring-channels with wide voids (16.4 × 8.0 Å), filled only by crystallization water, which are labile enough to be exchanged. Studies are in hand to investigate the solid

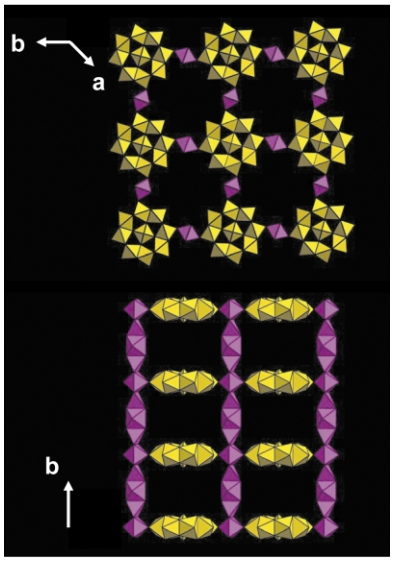

Fig. 15 View of the grid resulting from the anion–cation connections in the (010) plane (top) and view of the packing highlighting the Li^+ pillars in the [010] direction (bottom).

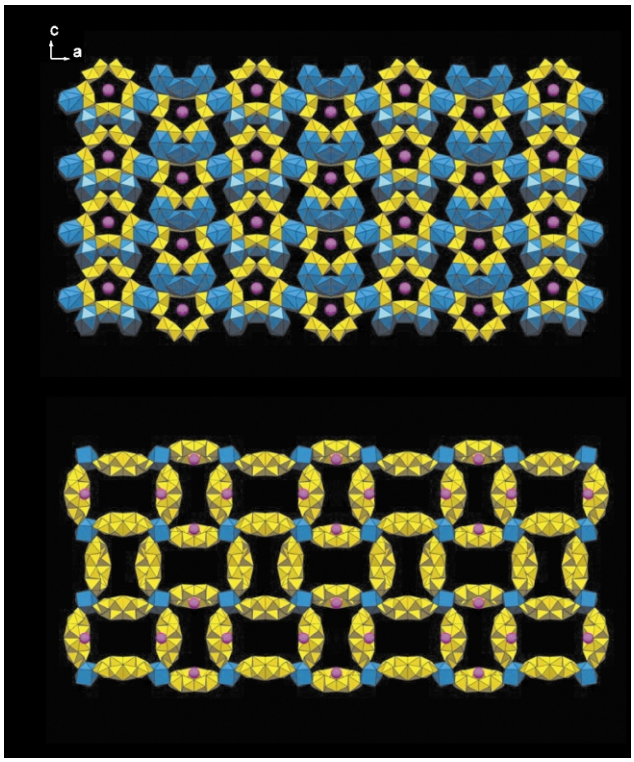

Fig. 16 Structure of $K_3[ClMo_{10}S_{10}O_{10}(OH)_{12}(H_2O)_3]\cdot 14H_2O$: (top) along the (010) plane, view of a potassium polyhedra layer paved by the ten-metal ring $[ClMo_{10}S_{10}O_{10}(OH)_{12}(H_2O)_3]^{3-}$; (bottom) *ad infinitum* grid parallel to the (001) plane, showing the wide open channels (16.4 × 8.0 Å).

state properties for K_3**4**$\cdot 14H_2O$ such as thermal stability, water removal and BET surface area measurements.

Outlook

We were gratified to realize that the $[M_2O_2S_2]^{2+}$ cation, an old and well-known conventional system, could be such a versatile and powerful tool for the elucidation of an original series of compounds. Here, a highly successful strategy was described, in terms of a *'building block approach'*. Hence, cyclic oxothiometalates represent an important new class of compounds in the wide field of the early transition-metal polyoxometalates. The initial fundamental chemistry controlling their formation are laid. The syntheses are facile: the crude parent precursor can be synthesized on a sixty gram scale and nearly all the derived compounds are obtained by simply mixing the precursor and the adequate template in water! Additionally, yields are quantitative in most cases. The chemical profiles of this aesthetically attractive collection of ring compounds has been investigated. For example, the cavity exhibits two types of behavior, which govern their reactivity toward anionic reagents: 'soft' bases such as halides weakly interact with polarized inner water molecules giving supramolecular complexes while stronger basic reagents are covalently encapsulated within the cavity. We look forward to continuing this fundamental development with special attention on how we might usefully apply these cycle-based properties in areas such as anion complexation, recognition and template synthesis. The use of specific organic guest molecules should be the key for the building up of increasingly sophisticated compounds, playing decisive roles in anionic recognition or in supramolecular structure formation. Furthermore, the possibility to enclose, confine or to exchange several molecules of substrate in the ring *in situ* offers some perspectives in the field of homogeneous catalysis, with the inorganic ring cluster playing the role of a molecular reactor.

Acknowledgments

We esspecially thank Jéîome Marrot for X-ray crystallograhic studies. We are indebted to Virginie Bereau, Bianca Marg, Sandra Riedel and Bernadette Salignac for their invaluable work in this domain. We are also grateful to Dr Anne Dolbecq for her significant input to this project.

Notes and references

1 C. Simonnet-Jégat and F. Sécheresse, *Chem. Rev.*, 2001, **9**, 2601–2611.
2 (*a*) D. Coucouvanis, *Adv. Inorg. Chem.*, 1998, **45**, 1; (*b*) E. I. Stiefel, *In Transition Metal Sulfur Chemistry, Biological and Industrial Signifiance*, ed. E. I. Stiefel and K. Matsumoto, ACS Symposium Series 653, American Chemical Society, Washington, DC, 1996, pp. 2–38.
3 *Molybdenum Enzymes*, ed. T. G. Spiro, Wiley, New York, 1985.
4 *Molybdenum Enzymes, Cofactors and Model Systems*, ed. E. I. Stiefel, D. Coucouvanis and W. E. Newton, ACS Symposium Series 535, American Chemical Society, Washington DC, 1993.
5 (*a*) H. Topsoe and B. S. Clausen, *Catal. Rev.-Sci. Eng.*, 1984, **26**, 395; (*b*) R. R. Chianelli, M. Daage and M. J. Ledoux, *Adv. Catal.*, 1994, **40**, 177.
6 (*a*) D. A. Vivic and W. D. Jones, *J. Am. Chem. Soc.*, 1999, **121**, 7606; (*b*) K. M. K. Dailey, T. B. Rauchfuss, A. L. RheingoldG and P. Yap, *J. Am. Chem. Soc.*, 1995, **117**, 6396; (*c*) A. J. Arce, Y. De Sanctis, A. Karam and A. J. Deeming, *Angew. Chem., Int. Ed. Engl.*, 1994, **116**, 1459.
7 T. Shibahara, *Coord. Chem. Rev.*, 1993, **123**, 73–147.
8 *Chem. Rev.*, ed. C. H. Hill, 1998, **98**.
9 (*a*) M. Misono, *Chem. Commun.*, 2001, 1441–1151; (*b*) N. Mizuno and M. Mizono, *Chem. Rev.*, 1998, **98**, 199; (*c*) T. Okuhara, N. Mizuno and M. Misono, *Adv. Catal.*, 1996, **41**, 113–252.
10 J. T. Rhule, C. L. Hill and D. A. Judd, *Chem. Rev.*, 1998, **98**, 327–357.
11 D. Katsoulis, *Chem. Rev.*, 1998, **98**, 359–387.
12 A. Müller, S. Q. N. Shah, H. Bögge and Schimdtmann, *Nature*, 1999, **397**, 48.
13 K. Wassermann, M. H. Dickman and M. T. Pope, *Angew. Chem., Int. Ed. Engl.*, 1997, **36**, 1445.
14 A. Müller, H. Reuter and S. Dillinger, *Angew. Chem., Int. Ed. Engl.*, 1995, **34**, 2328–2361.
15 W. G. Klemperer and C. Schwartz, *Inorg. Chem.*, 1985, **24**, 4459.
16 E. Cadot, V. Béreau and F. Sécheresse, *Inorg. Chim. Acta*, 1995, **239**, 39.
17 E. Radko, Y. J. Lu and R. H. Beer, *Inorg. Chem.*, 1996, **35**, 551.
18 E. Cadot, V. Béreau, S. Halut and F. Sécheresse, *Inorg. Chem.*, 1996, **95**, 551.

19 E. Cadot, B. Salignac, A. Dolbecq and F. Sécheresse, *Polyoxometalates Chemistry*, ed. M.T. Pope and A. Müller, Kluwer, Netherlands, 2001.
20 (*a*) B. Spivack and Z. Dori, *J. Am. Chem. Soc.*, 1971, **93**, 5265; (*b*) B. Spivack and Z. Dori, *Inorg. Nucl. Chem. Lett.*, 1975, **11**, 501.
21 E. Cadot, V. Béreau and F. Sécheresse, *Inorg. Chim. Acta*, 1996, **252**, 101–106.
22 V. Béreau, E. Cadot, H. Bögge, A. Müller and F. Sécheresse, *Inorg. Chem.*, 1996, **38**, 551.
23 A. Müller, V. P. Fedin, C. Khulmann, H. D. Fenske, G. Baum, H. Bögge and B. Hauptfleisch, *Chem. Commun.*, 1999, 1189.
24 M. T. Pope, *Hetero and Isopoly Oxometalates*, Springer-Verlag, New York, 1983.
25 (*a*) D. Coucouvanis, A. Toupadakis, S. M. Koo, C. G. Kim and A. Hadjikyriacou, *J. Am. Chem. Soc.*, 1991, **113**, 5271–5282; (*b*) R. Bhattacharyya, P. K. Chakrabarty, P. N. Ghosh, A. K. Mukherjee, D. Podder and M. Mukherjee, *Inorg. Chem.*, 1991, **30**, 3948–3955.
26 A. Mederos, D. M. Saysell, J. Sanchiz and A. G. Sykes, *J. Chem. Soc., Dalton Trans.*, 1998, 2723–2725.
27 (*a*) R. C. Haushalter and F. W. Lai, *Angew. Chem., Int. Ed. Engl.*, 1989, **28**, 743; (*b*) R. C. Haushalter and F. W. Lai, *Inorg. Chem.*, 1989, **28**, 2905.
28 (*a*) L. A. Mundi and R. C. Haushalter, *Inorg. Chem.*, 1992, **31**, 3050; (*b*) L. Meyer and R. C. Haushalter, *Inorg. Chem.*, 1993, **32**, 1579; (*c*) M. I. Khan, Q. Chen and J. Zubieta, *Inorg. Chim. Acta*, 1995, **235**, 135.
29 A. Müller, F. Peters, M. T. Pope and D. Gatteschi, *Chem. Rev.*, 1998, **98**, 239–271.
30 B. Spivack and Z. Dori, *J. Chem. Soc., Chem. Commun.*, 1973, 909.
31 T. Shibahara and H. Akashi, *Inorg. Synth.*, 1992, 254.
32 D. Coucouvanis, A. Toupadakis and A. Hadjikyriacou, *Inorg. Chem.*, 1988, **27**, 3272.
33 A. Müller, E. Krickmeyer and U. Reinsch, *Z. Anorg. Allg. Chem.*, 1980, **470**, 35–38.
34 A. Müller, W. Rittner, A. Neumann and R. C. Sharma, *Z. Anorg. Allg. Chem.*, 1981, **472**, 69–74.
35 J-P. Jolivet, *Metal Oxide Chemistry and Synthesis, From Solution to Solid State*, J. Wiley & Sons, Ltd, Chichester, 2000.
36 E. Cadot, B. Salignac, S. Halut and F. Sécheresse, *Angew. Chem., Int. Ed.*, 1998, **37**, 611.
37 E. Cadot, B. Salignac, J. Marrot, A. Dolbecq and F. Sécheresse, *Chem. Commun.*, 2000, 261–262.
38 E. Cadot, A. Dolbecq, B. Salignac and F. Sécheresse, *J. Phys. Chem. Solids*, 2001, **62**, 1533–1543.
39 B; Salignac, S. Riedel, A. Dolbecq, F. Sécheresse and E. Cadot, *J. Am. Chem. Soc.*, 2000, **122**, 10381–10389.
40 A. Dolbecq, E. Cadot and F. Sécheresse, *C. R. Acad. Sci. Paris, Sér. IIc*, 2000, **3**, 193–197.
41 C. Boskovic, M. Sadek, R. T. C. Brownlee, A. Bond and A. G. Wedd, *Chem. Commun.*, 1999, 533–534.
42 A. Dolbecq, B. Cadot, E. Cadot and F. Sécheresse, *Bull. Pol. Acad. Sci. Chem.*, 1998, **46**, 237–271.
43 E. Cadot, J. Marrot and F. Sécheresse, *Angew. Chem., Int. Ed.*, 2001, **40**, 774–777.
44 E. Cadot, B. Salignac, T. Loiseau, A. Dolbecq and F. Sécheresse, *Chem. Eur. J.*, 1999, **5**, 3390.
45 E. Cadot, A. Dolbecq, B. Salignac and F. Sécheresse, *Chem. Eur. J.*, 1999, **5**, 2396.
46 A. Dolbecq, E. Cadot, D. Eisner and F. Sécheresse, *Inorg. Chim. Acta*, 2000, **300-302**, 151–157.
47 L. C. W. Baker and J. S. J. Figgis, *J. Am. Chem. Soc.*, 1970, **92**, 3794.
48 J. F. Keggin, *Nature*, 1933, **131**, 908.
49 J. W. Akitt, N. N. Greenwood, B. L. Khandelwal and G. D. Lester, *J. Chem. Soc., Dalton Trans.*, 1972, 604.
50 H. K. Chae, W. G. Klemperer, D. E. Paez Loyo, V. W. Day and T. A. Eberspacher, *Inorg. Chem.*, 1992, **31**, 3189.
51 M. I. Khan, A. Müller, S. Dillinger, H. Bögge, Q. Chen and J. Zubieta, *Angew. Chem., Int. Ed. Engl.*, 1993, **32**, 1780.
52 A. Dolbecq, B. Salignac, E. Cadot and F. Sécheresse, *Chem. Commun.*, 1998, 2293.
53 A. Dolbecq, C. du Peloux, A.-L. Auberty, S. A. Mason, P. Barboux, J. Marrot, E. Cadot and F. Sécheresse, *Chem. Eur. J.*, 2002, **8**, 349–356.
54 E. Cadot, J. Marrot and F. Sécheresse, *J. Cluster Sci.*, 2002.
55 F. Sécheresse, E. Cadot and A. Dolbecq, *J. Solid State Chem*, 2000, **152**, 78–86.
56 A. D. Robertson, A. R. West and A. C. Ritchie, *Solid State Ionics*, 1997, **104**, 1.